

Nonreciprocity of supercurrent along applied magnetic field

Filippo Gaggioli,^{1,*} Yasen Hou,² Jagadeesh S. Moodera,^{2,1} and Akashdeep Kamra³

¹*Department of Physics, Massachusetts Institute of Technology, Cambridge, MA-02139, USA*

²*Francis Bitter Magnet Laboratory & Plasma Science and Fusion Center,
Massachusetts Institute of Technology, Cambridge, MA-02139, USA*

³*Condensed Matter Physics Center (IFIMAC) and Departamento de Física Teórica de la Materia Condensada,
Universidad Autónoma de Madrid, E-28049 Madrid, Spain*

Nonreciprocal current responses arise in a broad range of systems, from magnons and phonons to supercurrents, due to an interplay between spatial and temporal symmetry breakings. These find applications in devices, such as circulators and rectifiers, as well as in probing the interactions and states that underlie the nonreciprocity. An established symmetry argument anticipates emergence of nonreciprocal currents along a direction perpendicular to the applied magnetic field that breaks the time-reversal symmetry. Here, motivated by recent experiments, we examine the emergence of nonreciprocity in vortex-limited superconducting critical currents along an applied magnetic field. Employing London's equations for describing the Meissner response of a superconducting film, we find that an additional symmetry breaking due to a preferred vortex axis enables nonreciprocal critical currents along the applied magnetic field, consistent with the so far unexplained experimental observation. Building on our concrete theoretical model for supercurrents, we discuss a possible generalization of the prevailing symmetry consideration to encompass nonreciprocal currents along the time-reversal symmetry breaking direction.

Introduction.—When forward and backward directions can be distinguished in a system, nonreciprocal behavior can manifest via, for example, different resistances or currents along these opposite directions [1, 2]. A prototypical example is a p-n junction diode in which a simple identification of p-type and n-type subsystems admits different backward and forward current flows. Thus, in such systems divisible into two “lumped” subsystems, the spatial-inversion breaking along a direction \hat{n} alone can be sufficient to realize nonreciprocal behavior along this same axis [3–6]. In extended systems, one may distinguish between forward and backward transport along the axis $\hat{n} \times \hat{h}$, where \hat{h} is the direction of time-reversal symmetry breaking via an applied magnetic field or similar [7–9]. Consistent with this principle, nonreciprocal responses of magnons [10–13], phonons [14, 15], and Cooper pairs [16–20] perpendicular to an applied magnetic field have been observed using a wide range of systems and mechanisms [1, 2]. Such responses enable useful devices, such as rectifiers and circulators. At the same time, they offer a convenient probe for unconventional interactions and states of quantum matter [21–24]. Both these tasks, namely design of devices and effective probing, strongly rely on a general understanding of the symmetries that allow for nonreciprocal responses [2, 25, 26].

It therefore came as a surprise when unequal superconducting critical currents in the forward and backward directions, a phenomenon dubbed the superconducting diode effect (SDE) [16, 20], were observed in thin film superconductors subjected to a magnetic field *parallel* to the current flow direction [19], because the observation defied the symmetry-based expectation stated above. The phenomenon of SDE has gained a renewed interest [9, 27–29] and focus in the recent years due to its observation via a broad range of systems and mech-

anisms [16–20]. We here focus on thin films of a nominally centrosymmetric superconductor, where the time-reversal and spatial-inversion symmetries are broken, respectively, by an applied magnetic field and by inequivalent vortex surface barriers on the two sides [27, 30–32], possibly due to defects and geometric features introduced during the lithography process [19, 29]. The critical current in such thin films is typically determined by the Bean-Livingston vortex surface barrier [33]. The current which is large enough to exert sufficient Lorentz force on the vortices to overcome the weakest surface barrier becomes the critical value [31, 34–36] (Fig. 1). The consequent vortex-mediated SDE has been investigated and understood for applied magnetic fields perpendicular to the current flow direction [19, 29, 37–39], consistent with the prevailing symmetry argument above.

In this Letter, we examine the critical currents and SDE in a conventional centrosymmetric superconductor film subjected to a magnetic field parallel to the current flow direction, thereby going beyond the usual symmetry consideration. Considering the surface barrier mechanism typical of superconducting thin films [32], we find that the critical current is determined by the penetration of vortices whose axis is (weakly) tilted in the applied field direction. A surface barrier that is maximal for vortices with a finite tilt angle then gives rise to different critical currents in the forward and backward directions [Fig. 1 (b)]. Such an angular dependence for the vortex barrier may result from, for example, (controllable) geometrical defects induced by lithographic preparation of the film. Our theoretical results agree with the experimental data [19] semi-quantitatively and thus offer a plausible explanation. We further discuss a possible generalization of the prevailing symmetry argument and find nonreciprocity along the direction $\hat{n} \times V_0 \hat{h}$, where

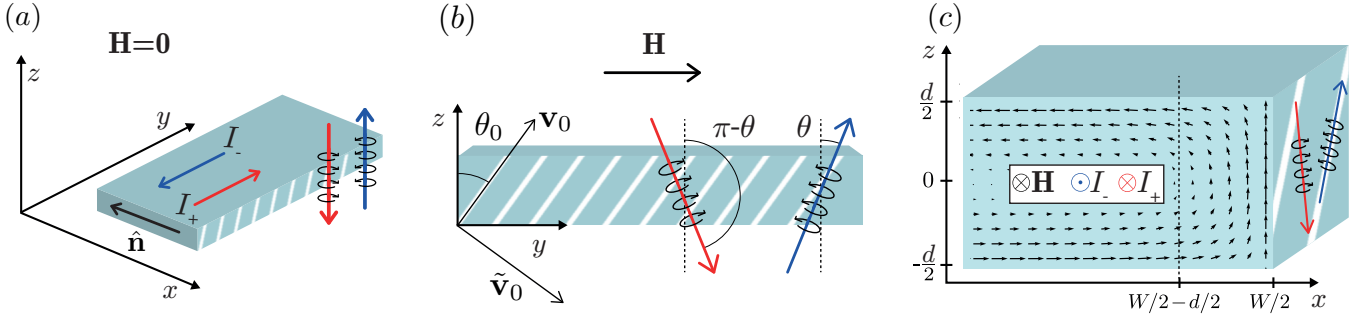


FIG. 1. Schematic depiction of the vortex mechanism underlying the SDE in an in-plane magnetic field \mathbf{H} parallel to the applied bias current \mathbf{I} . (a) For $\mathbf{H} = 0$, vortices penetrate the superconductor edges with their axes out-of-plane. For a sample with asymmetry along the $\hat{\mathbf{n}}$ direction, the right surface barrier, for example, is weaker and the vortices preferably penetrate from this edge with their axis (anti-)parallel to the z -axis for negative (positive) currents, thereby determining $I_c^\pm(0)$. (b) At finite \mathbf{H} , the vortices tilt in the direction of the magnetic field and form an angle θ ($\pi - \theta$) with the z -axis for negative (positive) currents. When the surface barrier is angular dependent and strongest (or weakest) along \mathbf{v}_0 ($\tilde{\mathbf{v}}_0$), e.g., because of the lithographic process (white stripes), the different barriers experienced by the tilted vortices result in unequal critical current densities for positive and negative current flows, giving rise to the SDE. (c) The current density across a xz -section of the thin film close to the right edge. This Meissner response to \mathbf{H} is given by Eq. (5) (for the z -component).

V_0 is a tensor characterizing the vortex barrier angular anisotropy. This reduces to the standard $\hat{\mathbf{n}} \times \hat{\mathbf{h}}$ framework when the vortex barrier has no angular dependence.

Vortex-limited critical current.— In a wide range of superconducting films, the critical supercurrent is determined by the presence of a steep surface barrier preventing the penetration of vortices inside the sample [32, 34–36, 40, 41]. This barrier is first overcome when the average Lorentz force density $\bar{\mathbf{F}}_L$ acting on the vortices – whose axis is not necessarily parallel to the out-of-plane direction [31] – reaches a critical value, associated to an equivalent critical current density j_s . For a thin film of width $-W/2 \leq x \leq W/2$ that extends indefinitely along y , this critical condition reads

$$\bar{\mathbf{F}}_L \left(\pm \frac{W}{2} \right) = \left(\frac{\phi_0}{c} \right) \bar{\mathbf{j}} \times \hat{\mathbf{e}}_v = \mp \left(\frac{\phi_0}{c} \right) j_s \hat{\mathbf{x}}, \quad (1)$$

for the vortex axis $\hat{\mathbf{e}}_v = (0, \sin\theta, \cos\theta)$ that maximizes the Lorentz force working against the surface barrier [31, 34]. Here, we denote the current density \mathbf{j} averaged over the coherence length ξ by $\bar{\mathbf{j}}$, $\phi_0 = hc/2e$ is the flux quantum. The task at hand is therefore to calculate the average current density $\bar{\mathbf{j}}$ flowing at distances $\lesssim \xi$ from the superconductor edges. Vortices with axis $\hat{\mathbf{e}}_v \perp \bar{\mathbf{j}}$ will then be the first to fulfill the condition (1), thereby determining $I_c(H)$.

In the absence of trapped vortices, the current density \mathbf{j} inside the superconductor is determined self-consistently by the interplay of the external field \mathbf{H} and the self-field produced by the current. In thin films with thickness d much smaller than the London length λ , the self-field is negligible [32] and the magnetic field is approximately constant inside and outside the superconductor. In this case, the current density distribution is

found from the London equation [32, 34]

$$\nabla \times \mathbf{j} = -\frac{c}{4\pi\lambda^2} \mathbf{H}, \quad (2)$$

with the additional condition that the integral $\int j_y dx dz$ is equal to the applied bias current $\mathbf{I} \parallel \hat{\mathbf{y}}$.

The solution to Eq. (2) depends on the magnetic field, the bias current and, via the vanishing of the current density j_\perp at the boundaries, on the precise film geometry. For a perpendicular magnetic field along the z axis, Eq. (2) yields x -dependent current density along y ,

$$j_y(x) = \frac{I}{dW} - \frac{c}{4\pi\lambda^2} Hx. \quad (3)$$

Following the principle described via Eq. (1), vortices enter the superconductor when the condition $j_y(x) = j_s$ is first met on either side of the film ($x = \pm W/2$): at zero magnetic field (external bias), this happens when the external bias (magnetic field) reaches [32]

$$I_0 \equiv j_s dW, \quad H_s \equiv \frac{8\pi\lambda^2}{cW} j_s. \quad (4)$$

In the parallel field scenario presented in Fig. 1(b), on the other hand, the bias current determines $j_y = \bar{j}_y = I/dW$, while the screening currents $\propto H$ flow in the xz -plane [Fig. 1(c)] with boundary conditions $j_x(x = \pm W/2, z) = j_z(x, z = \pm d/2) = 0$. The evaluation of these Meissner currents is detailed in the Appendix. For a small aspect ratio $d/W \ll 1$, we then find that

$$j_z(x, z) \approx \pm \frac{c}{4\pi\lambda^2} Hd \left(\sum_{n=0}^{\infty} \frac{(-1)^n}{(k_n d/2)^2} e^{-k_n \Delta x} \cos k_n z \right), \quad (5)$$

with $k_n = (n+1/2) 2\pi/d$ and $\Delta x = |W/2 \mp x|$ the distance from the edges. As expected, j_z grow rapidly at distances

$\lesssim d/2$ from the edges, where the effect of the boundary conditions $\mathbf{j} \perp \hat{\mathbf{x}}$ is important.

To average j_z over the size ξ of the vortex core, we take advantage of the rapid decay of the sum in Eq. (5) and consider only the contribution of the first (dominant) term to \bar{j}_z . For the typical thin films where $\pi\xi/d \gg 1$, this gives

$$\bar{j}_z \approx \pm \frac{2d}{\xi} \left(\frac{2}{\pi^2} \right)^2 \frac{c}{4\pi\lambda^2} Hd. \quad (6)$$

Using that $\hat{\mathbf{e}}_v \perp \bar{\mathbf{j}}$ for maximal Lorentz force and inserting the expressions for \bar{j}_y, \bar{j}_z , the condition (1) then provides an equation for $I_c(H)$,

$$\sqrt{\left(\frac{I_c(H)}{dW} \right)^2 + \left(\frac{2d}{\xi} \left(\frac{2}{\pi^2} \right)^2 \frac{c}{4\pi\lambda^2} Hd \right)^2} = j_s. \quad (7)$$

This finally yields the field dependence of the critical current

$$I_c(H) = I_0 \sqrt{1 - \left(\frac{H}{H_s^\parallel} \right)^2}, \quad (8)$$

with the characteristic field scale

$$H_s^\parallel = \left(\frac{\pi}{2} \right)^4 \left(\frac{\xi W}{d^2} \right) H_s, \quad (9)$$

that is directly related to the sample penetration field H_s in a perpendicular field [32]. Equations (8) and (9) show two interesting features that are in marked contrast with the $I_c(H)$ of the superconducting thin film in a perpendicular magnetic field. First, the field dependence is quadratic and not linear as for the perpendicular case [30, 32, 36]. Second, the magnetic scale H_s^\parallel is much larger than the corresponding H_s , as the prefactor in Eq. (9) is of the order of $\sim 10^4$ for $\xi/d \sim 1$ and a typical aspect ratio $d/W \sim 10^{-3}$. It then follows that an experiment measuring changes in the critical current for perpendicular fields in the order of Gauss should observe similar variations in $I_c(H)$ for parallel fields in the range of Tesla.

Having found the critical current (8), we fix $\bar{j}_x = I_c(H)$ and use that $\hat{\mathbf{e}}_v \perp \bar{\mathbf{j}}$ to evaluate the vortex tilt angles $\theta^{(L,R)}$ on the left and right edge

$$(\sin \theta^{(L,R)}, \cos \theta^{(L,R)}) = \left(\frac{H}{H_s^\parallel}, \pm \frac{I}{|I|} \sqrt{1 - \left(\frac{H}{H_s^\parallel} \right)^2} \right). \quad (10)$$

As shown in Fig. 1(b) and in agreement with the pseudovector properties of the magnetic field, the tilt angles at the two edges are exchanged upon switching the direction of the bias current I , such that $\theta^R \rightarrow \theta^L = \pi - \theta^R$.

Superconducting diode effect.— Let us now discuss the nonreciprocal transport properties of the parallel field

setup discussed above [19]. We first recapitulate the SDE in a perpendicular field, as this provides a useful comparison. The SDE, in the perpendicular case, is realized when the critical current densities $j_s^{(L,R)}$ on the left and right edge of the superconductor are not identical,

$$j_s^{(L,R)} = j_{s,0} \mp \Delta j_s (\hat{\mathbf{n}} \cdot \hat{\mathbf{x}}), \quad (11)$$

with Δj_s assumed positive, without a loss of generality, and the asymmetry vector $\hat{\mathbf{n}} = (-1, 0, 0)$ shown in Fig. 1(a). As a result, $I_c(H)$ reaches its maximum at the peak field [32]

$$\frac{H_{\max}}{H_{s,0}} = \frac{\Delta j_s}{j_{s,0}} \left[(\hat{\mathbf{n}} \times \hat{\mathbf{h}}) \cdot \hat{\mathbf{I}} \right], \quad (12)$$

which in turn determines the magnitude of the SDE.

In parallel in-plane fields, the magnitude of the current density $\bar{\mathbf{j}}$ at criticality is constant and determined by the weakest surface barrier. Vortices then always enter from the same edge, suggesting that no SDE can be realized in agreement with the fact that $\hat{\mathbf{n}} \times \hat{\mathbf{h}} = 0$. To understand the parallel-field SDE, we consider an additional kind of symmetry breaking, this time at the level of the individual surface barriers, that allows the system to distinguish between opposite signs of the bias current. We take into account a dependence of the surface barrier on the vortex tilt angle θ

$$j_s^{(L,R)}(\theta) = j_s^{(L,R)} + \delta j_s \cos 2(\theta_0 - \theta), \quad (13)$$

that may result, for example, from columnar tracks left by the lithographic process, represented as white stripes in Fig. 1. In assuming the form of this angular dependence, time-reversal symmetry requires the surface barrier to be the same for vortices with opposite fluxes. Considering reflections across the xz -plane, we then expect that the vortices will experience a different surface barrier (13) as $\theta \rightarrow \pi - \theta$ and $I \rightarrow -I$, giving rise to the SDE as long as $\theta_0 \neq 0, \pi/2$. In agreement with the time-reversal symmetry, SDE vanishes for $H = 0$ as the $\cos 2\theta$ dependence ensures that $j_s(\theta)$ remains the same when θ is changed from 0 to π .

In evaluating the critical condition (1) with $j_s(\theta)$ given by Eq. (13), we assume that the angular dependence is weak, i.e., $\delta j_s \ll j_s^{(L,R)}$, and much weaker than the difference between j_s^L and j_s^R , i.e., $\delta j_s \ll \Delta j_s$. This corresponds to the limit where vortex penetration happens from the weak (assumed right here) edge only, such that $j_s^R(\theta)$ alone determines the critical current $I_c(H)$ while $j_s^L(\theta)$ does not play any role. In what follows, we will therefore neglect the (L, R) indices unless necessary.

With the right tilt angle θ given by Eq. (10), the field dependence of the surface barrier (13) can be immediately found (we neglect terms $\propto (\delta j_s/j_s)^2$),

$$j_s(H) = j_s \left[1 + \frac{\delta j_s}{j_s} \cos \left(2\theta_0 \pm 2H/H_s^\parallel \right) \right], \quad (14)$$

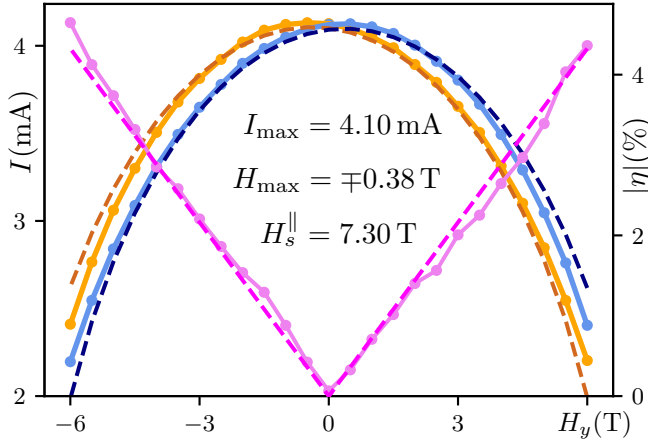


FIG. 2. Experimental data from Ref. 19 (circles and solid lines) for the critical current $I_c^\pm(H)$ (orange and blue) and the SDE efficiency $|\eta(H)|$ (pink) for a superconducting vanadium thin film in a parallel in-plane magnetic field. Fitting Eqs. (15) and (18) from our theoretical model (dashed lines), we find very good agreement for the indicated choice of parameters. The field $H_s^\parallel \approx 7.30$ T obtained from fitting agrees well with the prediction $H_s^\parallel \sim 9$ T from Eq. (9), using the experimental values for H_s, ξ, d and W from Ref. 19.

where the plus and minus signs refer to positive and negative bias currents. To determine $I_c(H)$ from Eq. (1), we now plug in (14) and expand the cosine term around $2\theta_0$ while neglecting terms $\propto (\delta j_s/j_s)^2$ and $\propto (\delta j_s/j_s)(H/H_s^\parallel)^2$ leading to

$$I_c^\pm(H) \approx I_{\max} \sqrt{1 - \left(\frac{H - H_{\max}^\pm}{H_s^\parallel} \right)^2}, \quad (15)$$

where we introduced the peak field

$$H_{\max}^\pm = \mp \left(2 \sin 2\theta_0 \frac{\delta j_s}{j_s} \right) H_s^\parallel, \quad (16)$$

and the peak current

$$I_{\max} = I_0 \sqrt{1 + \cot(2\theta_0) \frac{|H_{\max}^\pm|}{H_s^\parallel}}. \quad (17)$$

The shifted field dependence (15) results from the two-fold contributions of the magnetic field to vortex penetration: on the one hand, to enhance the Meissner current (6) and, on the other, to reinforce the surface barrier (14). These effects compensate at the peak field H_{\max} , which does not depend on the left-right asymmetry $\Delta j_s/j_{s,0}$, as in Eq. (12), but is fixed entirely by the parameters $\delta j_s/j_s$ and θ_0 in the limit where $I_c(H)$ is determined by the right edge alone.

As in the case of a perpendicular field, the peak field H_{\max} determines the efficiency η of the superconducting diode device $\eta(H) \equiv (I_c^+(H) - I_c^-(H)) / (I_c^+(H) + I_c^-(H))$.

Using Eq. (15) and neglecting terms $\propto (H_{\max}/H_s^\parallel)^2$ and $\propto (H_{\max}/H_s^\parallel)(H/H_s^\parallel)^3$, this is found to read

$$\eta(H) \approx \left(\frac{H_{\max}^+}{H_s^\parallel} \right) \frac{H}{H_s^\parallel}. \quad (18)$$

Equations (15) and (18) lend themselves conveniently to a comparison with the experimental results on the parallel-field SDE reported in Ref. 19. Fitting $I_c^\pm(H)$ and $\eta(H)$ to the experimental data, we obtain the dashed curves in Fig. 2. These reproduce the critical currents and the efficiency curve very well for the choice of $I_{\max}, H_{\max}, H_s^\parallel$ reported in the plot. The small differences can result from the various approximations employed in our analytic simplifications. This combination of parameters is consistent with the assumptions underlying Eqs. (15) and (18), as $(\delta j_s/j_s) \sim (H_{\max}^\pm/H_s^\parallel) \ll 1$.

Finally, we compare the field value $H_s^\parallel = 7.30$ T estimated from the fit in Fig. 2 to our theoretical prediction (9). Using the experimental value $H_s \approx 11$ Oe for the perpendicular penetration field and taking $\xi \approx 11$ nm, $d \approx 8$ nm and $W = 8 \mu\text{m}$ from Ref. 19, we find that $H_s^\parallel \sim 9$ T, in satisfactory agreement with the result of our fit.

Generalized symmetry indicator for nonreciprocity.— Building upon the insights gained from our theoretical model of the SDE in a magnetic field applied along the current flow direction [19], we now discuss an appropriate generalization of $\hat{\mathbf{n}} \times \hat{\mathbf{h}}$ as the direction of nonreciprocity. The crucial addition comes from the angular dependence of the vortex surface barrier. Our model suggests that we should find SDE whenever the vortex tilting due to the applied magnetic field causes the vortices to experience different surface barriers for forward and backward current flows. This general idea supersedes the simple case of applied magnetic field along the current direction, as we now formulate.

As discussed below Eq. (13), the surface barrier needs to satisfy time-reversal symmetry and thus remain the same when $\theta \rightarrow \theta + \pi$. For this reason, the symmetry-breaking associated with angular dependence $j_s(\theta)$ cannot be parametrized by a simple vector, as was the case for the left-right asymmetry (11), but requires the introduction of a tensor quantity $V_0 = \mathbf{v}_0 \mathbf{v}_0^T - \tilde{\mathbf{v}}_0 \tilde{\mathbf{v}}_0^T$, built from the vectors $\mathbf{v}_0 = (0, \sin \theta_0, \cos \theta_0)$ and $\tilde{\mathbf{v}}_0 = (0, \cos \theta_0, -\sin \theta_0)$ that constitute the symmetry axes of the angular dependence [see Eq. (13) and Fig. 1(b)]. In terms of V_0 , the surface barrier (13) reads

$$j_s^{(L,R)}(\theta) = j_s^{(L,R)} + \delta j_s (\hat{\mathbf{e}}_v V_0 \hat{\mathbf{e}}_v), \quad (19)$$

such that Eqs. (16) and (18) take the simple form

$$\eta(H) \propto \frac{H_{\max}}{H_s^\parallel} = \frac{2\delta j_s}{j_s} \left[(\hat{\mathbf{n}} \times V_0 \hat{\mathbf{h}}) \cdot \hat{\mathbf{I}} \right]. \quad (20)$$

The peak field (20) is maximal when $\hat{\mathbf{h}}$ is parallel to $\hat{\mathbf{I}}$, and vanishes when they are orthogonal. The structure of

Eqs. (19) and (20), however, suggests that this is just a special case. Considering now edges that are tilted by an angle ϕ away from the z -axis in the xz -plane, such that $(\mathbf{v}_0, \hat{\mathbf{v}}_0) \rightarrow R_y(\phi)(\mathbf{v}_0, \hat{\mathbf{v}}_0)$ with the matrix $R_y(\phi)$ describing rotations about the y -axis, we find that the tensor V_0 transforms as $R_y(\phi)V_0R_y^T(\phi)$. Inserting this into Eq. (20) then allows to evaluate H_{\max} for an arbitrary direction of the in-plane field $\hat{\mathbf{h}} = (h_x, h_y, 0)$

$$\frac{H_{\max}}{H_s^{\parallel}} = \frac{2\delta j_s}{j_s} [h_y \sin 2\theta_0 + h_x \sin \phi \cos 2\theta_0] \cos \phi, \quad (21)$$

with the SDE efficiency $\eta(H)$ again $\propto H_{\max}/H_s^{\parallel}$. This further admits finite SDE when magnetic field is applied along an arbitrary in-plane direction and is consistent with the experiments [19] similar to those discussed in Fig. 2 when the field is applied along the x -axis.

Conclusion.— Our theoretical treatment of vortex-limited superconducting critical current offers a possible explanation for, and a good agreement with, the experimentally observed SDE in superconducting thin films subjected to in-plane magnetic fields, especially along the current flow direction. It further suggests new avenues for a lithographic control of the SDE via the angle θ_0 . Our consequent generalization of the symmetry arguments for observing nonreciprocity offers an important supplement to the existing understanding and may guide similar search for nonreciprocal responses in other non-superconductor systems.

Acknowledgements.— F.G. is grateful for the financial support from the Swiss National Science Foundation (Postdoc.Mobility Grant No. 222230) and the support of the EU Cost Action CA16218 (NANOCOHYBRI). A.K. acknowledges financial support from the Spanish Ministry for Science and Innovation – AEI Grant CEX2018-000805-M (through the “Maria de Maeztu” Programme for Units of Excellence in R&D) and grant RYC2021-031063-I funded by MCIN/AEI/10.13039/501100011033 and “European Union Next Generation EU/PRTR”. The work at J.S.M Lab was supported by Air Force Office of Sponsored Research (FA9550-23-1-0004 DEF), Office of Naval Research (N00014-20-1-2306), National Science Foundation (NSF-DMR 1700137 and 2218550); the Army Research Office (W911NF-20-2-0061 and DURIP W911NF-20-1-0074) and the Center for Integrated Quantum Materials (NSF-DMR 1231319).

* Corresponding author. Email: gflipppo@mit.edu

- [1] Y. Tokura and N. Nagaosa, Nonreciprocal responses from non-centrosymmetric quantum materials, *Nature Communications* **9**, 3740 (2018).
 [2] N. Nagaosa and Y. Yanase, Nonreciprocal transport and optical phenomena in quantum materials, *Annual Review of Condensed Matter Physics* **15**, 63 (2024).

- [3] J. Hu, C. Wu, and X. Dai, Proposed design of a Josephson diode, *Phys. Rev. Lett.* **99**, 067004 (2007).
 [4] E. Strambini, M. Spies, N. Ligato, S. Ilić, M. Rouco, C. González-Orellana, M. Ilyn, C. Rogero, F. S. Bergeret, J. S. Moodera, P. Virtanen, T. T. Heikkilä, and F. Giazotto, Superconducting spintronic tunnel diode, *Nature Communications* **13**, 2431 (2022).
 [5] M. Amundsen, I. V. Bobkova, and A. Kamra, Magnonic spin joule heating and rectification effects, *Phys. Rev. B* **106**, 144411 (2022).
 [6] Z. Geng, A. Hijano, S. Ilić, M. Ilyn, I. Maasilta, A. Monfardini, M. Spies, E. Strambini, P. Virtanen, M. Calvo, C. González-Orellana, A. P. Helenius, S. Khorsidian, C. I. L. de Araujo, F. Levy-Bertrand, C. Rogero, F. Giazotto, F. S. Bergeret, and T. T. Heikkilä, Superconductor-ferromagnet hybrids for non-reciprocal electronics and detectors, *Superconductor Science and Technology* **36**, 123001 (2023).
 [7] G. L. J. A. Rikken, J. Fölling, and P. Wyder, Electrical magnetochiral anisotropy, *Phys. Rev. Lett.* **87**, 236602 (2001).
 [8] G. L. J. A. Rikken, C. Strohm, and P. Wyder, Observation of magnetoelectric directional anisotropy, *Phys. Rev. Lett.* **89**, 133005 (2002).
 [9] V. M. Edelstein, Spin polarization of conduction electrons induced by electric current in two-dimensional asymmetric electron systems, *Solid State Communications* **73**, 233 (1990).
 [10] N. Ogawa, L. Köhler, M. Garst, S. Toyoda, S. Seki, and Y. Tokura, Nonreciprocity of spin waves in the conical helix state, *Proceedings of the National Academy of Sciences* **118**, e2022927118 (2021), <https://www.pnas.org/doi/pdf/10.1073/pnas.2022927118>.
 [11] S.-H. Yang, R. Naaman, Y. Paltiel, and S. S. P. Parkin, Chiral spintronics, *Nature Reviews Physics* **3**, 328 (2021).
 [12] J. Gückelhorn, S. de-la Peña, M. Scheufele, M. Grammer, M. Opel, S. Geprägs, J. C. Cuevas, R. Gross, H. Huebl, A. Kamra, and M. Althammer, Observation of the non-reciprocal magnon Hanle effect, *Phys. Rev. Lett.* **130**, 216703 (2023).
 [13] T. Yu, Z. Luo, and G. E. Bauer, Chirality as generalized spin-orbit interaction in spintronics, *Physics Reports* **1009**, 1 (2023), chirality as Generalized Spin-Orbit Interaction in Spintronics.
 [14] M. Küß, M. Heigl, L. Flacke, A. Hörner, M. Weiler, M. Albrecht, and A. Wixforth, Nonreciprocal dzyaloshinskii-moriya magnetoacoustic waves, *Phys. Rev. Lett.* **125**, 217203 (2020).
 [15] M. Küß, M. Albrecht, and M. Weiler, Chiral magnetoacoustics, *Frontiers in Physics* **10**, 10.3389/fphy.2022.981257 (2022).
 [16] F. Ando, Y. Miyasaka, T. Li, J. Ishizuka, T. Arakawa, Y. Shiota, T. Moriyama, Y. Yanase, and T. Ono, Observation of superconducting diode effect, *Nature* **584**, 373 (2020).
 [17] C. Baumgartner, L. Fuchs, A. Costa, S. Reinhardt, S. Gronin, G. C. Gardner, T. Lindemann, M. J. Manfra, P. E. Faria Junior, D. Kochan, J. Fabian, N. Paradiso, and C. Strunk, Supercurrent rectification and magnetochiral effects in symmetric Josephson junctions, *Nature Nanotechnology* **17**, 39 (2022).
 [18] B. Pal, A. Chakraborty, P. K. Sivakumar, M. Davydova, A. K. Gopi, A. K. Pandeya, J. A. Krieger, Y. Zhang, M. Date, S. Ju, N. Yuan, N. B. Schröter, L. Fu, and

- S. S. Parkin, Josephson diode effect from cooper pair momentum in a topological semimetal, arXiv:2112.11285 (2021).
- [19] Y. Hou, F. Nichele, H. Chi, A. Lodesani, Y. Wu, M. F. Ritter, D. Z. Haxell, M. Davydova, S. Ilić, O. Glezakou-Elbert, A. Varambally, F. S. Bergeret, A. Kamra, L. Fu, P. A. Lee, and J. S. Moodera, Ubiquitous superconducting diode effect in superconductor thin films, *Physical Review Letters* **131**, 027001 (2023).
- [20] M. Nadeem, M. S. Fuhrer, and X. Wang, The superconducting diode effect, *Nature Reviews Physics* **5**, 558 (2023).
- [21] N. F. Q. Yuan and L. Fu, Supercurrent diode effect and finite-momentum superconductors, *Proceedings of the National Academy of Sciences* **119**, e2119548119 (2022).
- [22] A. Daido, Y. Ikeda, and Y. Yanase, Intrinsic superconducting diode effect, *Phys. Rev. Lett.* **128**, 037001 (2022).
- [23] J. J. He, Y. Tanaka, and N. Nagaosa, A phenomenological theory of superconductor diodes, *New Journal of Physics* **24**, 053014 (2022).
- [24] S. Ilić and F. S. Bergeret, Theory of the supercurrent diode effect in rashba superconductors with arbitrary disorder, *Phys. Rev. Lett.* **128**, 177001 (2022).
- [25] B. Zinkl, K. Hamamoto, and M. Sigrist, Symmetry conditions for the superconducting diode effect in chiral superconductors, *Physical Review Research* **4**, 033167 (2022).
- [26] P. J. W. Moll and V. B. Geshkenbein, Evolution of superconducting diodes, *Nature Physics* **19**, 1379 (2023).
- [27] D. Y. Vodolazov and F. M. Peeters, Superconducting rectifier based on the asymmetric surface barrier effect, *Physical Review B* **72**, 172508 (2005).
- [28] D. Y. Vodolazov, B. A. Gribkov, S. A. Gusev, A. Y. Klimov, Y. N. Nozdrin, V. V. Rogov, and S. N. Vdovichev, Considerable enhancement of the critical current in a superconducting film by a magnetized magnetic strip, *Phys. Rev. B* **72**, 064509 (2005).
- [29] D. Cerbu, V. N. Gladilin, J. Cuppens, J. Fritzsche, J. Tempere, J. T. Devreese, V. V. Moshchalkov, A. V. Silhanek, and J. V. de Vondel, Vortex ratchet induced by controlled edge roughness, *New Journal of Physics* **15**, 063022 (2013).
- [30] B. L. T. Plourde, D. J. Van Harlingen, D. Y. Vodolazov, R. Besseling, M. B. S. Hesselberth, and P. H. Kes, Influence of edge barriers on vortex dynamics in thin weak-pinning superconducting strips, *Physical Review B* **64**, 014503 (2001).
- [31] M. K. Hope, M. Amundsen, D. Suri, J. S. Moodera, and A. Kamra, Interfacial control of vortex-limited critical current in type-II superconductor films, *Phys. Rev. B* **104**, 184512 (2021).
- [32] F. Gaggioli, G. Blatter, K. S. Novoselov, and V. B. Geshkenbein, Superconductivity in atomically thin films: 2d critical state model, (2024), arXiv:2402.07973 [cond-mat.supr-con].
- [33] C. P. Bean and J. D. Livingston, Surface barrier in type-II superconductors, *Physical Review Letters* **12**, 14 (1964).
- [34] V. V. Shmidt, The critical current in superconducting films, *Soviet Physics JETP* **30**, 1137 (1970).
- [35] V. V. Shmidt, Critical currents in superconductors, *Soviet Physics Uspekhi* **13**, 408 (1970).
- [36] G. M. Maksimova, Mixed state and critical current in narrow semiconducting films, *Physics of the Solid State* **40**, 1607 (1998).
- [37] D. Suri, A. Kamra, T. N. G. Meier, M. Kronseder, W. Belzig, C. H. Back, and C. Strunk, Non-reciprocity of vortex-limited critical current in conventional superconducting micro-bridges, *Applied Physics Letters* **121**, 102601 (2022).
- [38] A. Gutfreund, H. Matsuki, V. Plastovets, A. Noah, L. Gorzawski, N. Fridman, G. Yang, A. Buzdin, O. Millo, J. W. A. Robinson, and Y. Anahory, Direct observation of a superconducting vortex diode, *Nature Communications* **14**, 1630 (2023).
- [39] S. Chahid, S. Teknowijoyo, I. Mowgood, and A. Gulian, High-frequency diode effect in superconducting nb₃Sn microbridges, *Phys. Rev. B* **107**, 054506 (2023).
- [40] J. R. Clem, Josephson junctions in thin and narrow rectangular superconducting strips, *Physical Review B* **81**, 144515 (2010).
- [41] J. R. Clem and K. K. Berggren, Geometry-dependent critical currents in superconducting nanocircuits, *Physical Review B* **84**, 174510 (2011).
- [42] J. D. Jackson, *Classical electrodynamics*, 3rd ed. (Wiley, New York, NY, 1999).

Meissner currents distribution

In this Appendix, we determine the distribution of the screening currents j_x, j_z induced by an in-plane magnetic field applied parallel to the direction of the bias current. To do so, we treat the xz -section of the thin film as a two-dimensional superconductor of length W and width d , threaded by a perpendicular magnetic field in the y -direction, see Fig. 1(c) in the main text.

We then write the London equation for the current density \mathbf{j} in terms of the vector potential \mathbf{A} and the order parameter phase φ ,

$$\mathbf{j} = -\frac{c}{4\pi\lambda^2} \left[\mathbf{A} - \frac{\phi_0}{2\pi} \nabla\varphi \right] \quad (22)$$

with boundary conditions $j_x(x = \pm W/2, z) = j_z(x, z = \pm d/2) = 0$. Taking the curl of Eq. (22) reproduces Eq. (2) in the main text.

Having chosen the gauge $\mathbf{A} = -Hz\hat{\mathbf{x}}$, we use the incompressibility condition $\nabla \cdot \mathbf{j} = 0$ to obtain the Laplace equation $\nabla^2\varphi = 0$ with boundary conditions $\partial_z\varphi(x, z = \pm d/2) = 0$ and $\partial_x\varphi(x = \pm W/2, z) = +(2\pi/\phi_0)Hz$. The solution is then obtained by the method of separation of

variables [42] and reads (cf. Ref. 40)

$$\varphi(x, z) = \frac{8\pi H}{\phi_0 d} \sum_{n=0}^{\infty} \frac{(-1)^n \cosh(k_n x) \sin(k_n z)}{k_n^3 \cosh(k_n W/2)} \quad (23)$$

with $k_n = (n + 1/2)2\pi/d$. Eq. (23) satisfies the boundary conditions above, as can be proven with the help of Poisson's summation formula.

Taking the gradient of the phase (23) and inserting into Eq. (22), we obtain the screening current distribution shown in Fig. 1(c) in the main text. For a film with small aspect ratio $d/W \ll 1$, we expand the hyperbolic cosine and find

$$j_x \approx -\frac{c}{4\pi\lambda^2} Hd \left(\frac{z}{d} + \sum_{n=0}^{\infty} \frac{(-1)^n}{(k_n d/2)^2} e^{-k_n \Delta x} \sin k_n z \right), \quad (24)$$

$$j_z \approx \pm \frac{c}{4\pi\lambda^2} Hd \left(\sum_{n=0}^{\infty} \frac{(-1)^n}{(k_n d/2)^2} e^{-k_n \Delta x} \cos k_n z \right), \quad (25)$$

where the plus and minus signs refer to the right and left halves of the superconductor and $\Delta x = |W/2 \mp x|$ is the distance from the closest edge.